Anal. Chem. **2002,** *74,* 3690−3697

Fully Integrated On-Chip Electrochemical Detection for Capillary Electrophoresis in a Microfabricated Device

Richard P. Baldwin,*,§ Thomas J. Roussel, Jr.,† Mark M. Crain,‡ Vijay Bathlagunda,‡ Douglas J. Jackson,‡ Jayadeep Gullapalli,§ John A. Conklin,‡ Rekha Pai,‡ John F. Naber,‡ Kevin M. Walsh,‡ and Robert S. Keynton†

Department of Chemistry, University of Louisville, Louisville, Kentucky 40292, Department of Mechanical Engineering, University of Louisville, Louisville, Kentucky 40292 and Department of Electrical and Computer Engineering, University of Louisville, Louisville, Kentucky 40292

Microfabricated lab-on-a-chip devices employing a fully integrated electrochemical (EC) detection system have been developed and evaluated. Both capillary electrophoresis (CE) channels and all CE/EC electrodes were incorporated directly onto glass substrates via traditional microfabrication techniques, including photolithographic patterning, wet chemical etching, DC sputtering, and thermal wafer bonding. Unlike analogous CE/EC devices previously reported, no external electrodes were required, and critical electrode characteristics, including size, shape, and placement on the microchip, were established absolutely by the photolithography process. For the model analytes dopamine and catechol, detection limits in the 4−5 μM range (∼200 amol injected) were obtained with the Pt EC electrodes employed here, and devices gave stable analytical performance over months of usage.

One of the dominant themes in analytical instrumentation over the past decade has been the application of microfabrication techniques, common to the computer industry, to the design and construction of ultraminiaturized or "lab-on-a-chip" measurement systems.[1,2] On one hand, these devices can consist of sophisticated sample-holding platforms containing hundreds of microwells to facilitate screening of large sample populations or processing of special kinds of samples. On the other, they can aspire to be full analytical instruments (or even laboratories) capable of carrying out diverse functions, including not only sample detection but also sample treatment, separation, and collection processes, as well. Probably the most noteworthy practical examples reported so far for this microtechnology have involved its application for immunoassays[3] and DNA analysis[4−6] and sequencing.[7,8]

At the heart of the lab-on-a-chip concept is the use of photolithographic or micromachining techniques to construct precisely defined wells, channels, or other features onto either silicon-based, glass, or polymeric substrates. These structures, which form the basis of the chip's sample holding, transfer, and separation operations, are usually fabricated on the 10−100-μm scale and clearly are consistent with the creation of extremely small analysis devices. However, to realize fully the size-reduction potential of lab-on-a-chip devices, it is necessary to be able to construct equally miniaturized structures to carry out detection and other support functions. To date, lab-on-a-chip detection schemes have most often utilized laser-induced fluorescence (LIF) because of its high sensitivity and its compatibility with the typical chip dimensions cited above. However, despite the success that LIF has enjoyed with microfabricated instrumentation, it has normally been employed in an off-chip format in which the detection system itself is significantly larger. As a consequence, there have been few reported examples of fully miniaturized lab-on-a-chip systems that succeed in integrating the detection scheme directly onto the chip platform and realize the ultimate system size reduction.

Although LIF and other optical approaches have considerable potential for such on-chip integration,[9,10] a detection methodology that is more ideally suited to microfabrication would seem to be electrochemistry (EC). Conventional photolithographic techniques can readily produce micrometer-sized EC electrodes directly on a wide range of substrate materials by formation of conducting metal films via sputtering or vapor deposition. Thus, the incorporation of EC electrodes can be accomplished simply as an additional step in the microfabrication process. In addition, this approach also has the advantage that the specific electrode

* Fax: (502) 852-8149. E-mail address: rick.baldwin@louisville.edu.
† Department of Mechanical Engineering.
‡ Department of Electrical and Computer Engineering.
§ Department of Chemistry.

(1) Service, R. F. *Science* **1998**, *282*, 396−401.
(2) Figeys, D.; Pinto, D. *Anal. Chem.* **2000**, *72*, 330A−335A.
(3) Chiem, N.; Harrison, D. J. *Anal. Chem.* **1997**, *69*, 373−378.
(4) Woolley, A. T.; Mathies, R. A. *Proc. Natl. Acad. Sci. U.S.A.* **1994**, *91*, 11348−11352.
(5) Effenhauser, C. S.; Paulus, A.; Manz, A.; Widmer, H. M. *Anal. Chem.* **1994**, *66*, 2949−2953.
(6) Woolley, A. T.; Hadley, D.; Landre, P.; deMello, A. J.; Mathies, R. A.; Northrup, M. A. *Anal. Chem.* **1996**, *68*, 4081−4086.
(7) Woolley, A. T.; Mathies, R. A. *Anal. Chem.* **1995**, *67*, 3676−3680.
(8) Schmalzing, D.; Adourian, A.; Koutny, L.; Ziaugra, L.; Matsudaira, P.; Ehrlich, D. *Anal. Chem.* **1998**, *70*, 2303−2310.
(9) Burns, M. A.; Johnson, B. N.; Brahmasandra, S. N.; Handique, K.; Webster, J. R.; Krishnan, M.; Sammarco, T. S.; Man, P. M.; Jones, D.; Heldsinger, D.; Mastrangelo, C. H.; Burke, D. T. *Science* **1998**, *282*, 484−487.
(10) Chabinyc, M. L.; Chiu, D. T.; McDonald, J. C.; Stroock, A. D.; Christian, J. F.; Karger, A. M.; Whitesides, G. M. *Anal. Chem.* **2001**, *73*, 4491−4498.

10.1021/ac011188n CCC: $22.00
Published on Web 06/27/2002

features critical for optimum detector performance (e.g., the number of electrodes and their exact size, shape, and placement) can be precisely controlled during chip fabrication.

In the broadest sense, EC detection can be carried out in one of three different formats: conductivity, potentiometry, and amperometry. Although there have been a few reports in which the first two of these were successfully applied to microchip devices,[11] EC detection in the amperometric mode has been the most popular choice to date. This approach was first reported in 1998 by Woolley et al.,[12] who used photolithographically patterned Pt working and counter electrodes to detect catecholamines and DNA fragments amperometrically following separation by capillary electrophoresis (CE). Subsequently, there have been numerous reports that have demonstrated an increasing number of CE/EC applications for microchip devices.[13−23] In these reports, the specific electrode arrangements and microfabrication procedures employed have varied widely in nature. For example, Wang's approach[13−16] has been to pattern the CE channel all the way to the edge of the microchip and use off-chip EC electrodes mounted a short distance away in the CE buffer reservoir. However, most other groups have chosen to incorporate the EC working electrode directly onto the microchip. Usually this has been accomplished by microfabricating a cavity or trench near the end of the CE channel by photolithography or laser ablation. Following this, the electrodes were actually prepared by a manual operation in which a suitable conductive material was physically inserted into or applied onto the cavity, for example, Pt, Au, or C wires[17,19,23] and C ink.[20−22] In these cases, the microfabrication process served only to help locate the working electrode favorably on the chip. Chen et al.[24] have reported the thermal vapor deposition of a Pd film decoupler and working electrodes onto Plexiglas-based chips.

Despite these successes, it is surprising that complete advantage of microfabrication has not yet been taken to construct a fully integrated CE/EC device in which all EC and CE electrodes are patterned physically onto the microchip, and no external electrodes are required. Following Woolley's initial work with CE/EC microchips,[12] there has been only one instance subsequently reported in which the EC working electrodes were patterned directly onto the microchip photolithographically.[18] And in virtually all cases, other EC electrodes—reference and counter—as well as the CE anode and cathode have been completely conventional in size and design, consisting of ordinary Ag/AgCl or Pt wire electrodes that were manually inserted into the chip via appropriately located access holes.

This situation appears to be highly undesirable for several reasons. First, inclusion of all electrodes directly onto the chip surface is required to take full advantage of the microfabrication approach. Without this, additional manual operations are needed to complete construction of the device, and the "mass production" potential inherent to photolithographic fabrication is severely compromised. Second, from the work reported thus far,[12,14,22,23] it is apparent that electrode placement plays a significant role in determining instrument performance (e.g., background currents and potential control), and microfabrication of electrodes provides a far better opportunity to control and optimize all electrode features than does the manual approach. Finally, potential applications of lab-on-a-chip analysis devices involving remote (field) or on-site (physician's office) measurements outside the research laboratory require portable or transportable systems in which manipulation of external electrodes is not acceptable. In reality, broad usage of such devices beyond the specialized EC research community is highly unlikely to occur without the availability of ready-to-use, packaged analysis systems requiring no more than plug-in or software operations on the part of the end user.

Accordingly, our lab-on-a-chip efforts have been directed toward the development of self-contained and transportable CE/EC analysis systems that are consistent with the wide range of possible applications for these devices. This effort has consisted of two separate elements: (1) the design and characterization of microchips in which all CE and EC electrodes are incorporated directly onto the chip as part of the microfabrication process and (2) the design and construction of miniaturized CE and EC electronics needed to support these devices. This paper will describe our initial efforts directed toward the first of these objectives; the latter is discussed in a subsequent paper.[25]

EXPERIMENTAL SECTION

Microfabrication Procedures. The experimental CE/EC device, depicted in Figures 1 and 2, consisted of two soda lime glass substrates that were processed using traditional microfabrication techniques and then thermally bonded together. The glass substrates began as 5 cm × 3.5 cm ultraflat soda lime photomask blanks (Nanofilm, Inc., Westlake Village, CA) that were purchased precoated with a thin chrome layer and positive AZ1518 photoresist. The ultraflat surface of the photomask promoted effective leak-free bonding, and the soda lime composition allowed thermal bonding at a reduced temperature. These two properties were critical to the success of the final bonding process.

The bottom substrate contained the seven CE and EC electrodes, which were formed by a photolithographic liftoff process. The electrode pattern was first transferred onto the precoated resist layer using an appropriate darkfield chrome

(11) Guijt, R. M.; Baltussen, E.; van der Steen, G.; Schasfoort, R. B. M.; Schlautmann, S.; Billiet, H. A. H.; Frank, J.; van Dedem G. W. K.; van den Berg, A. *Electrophoresis* **2001**, *22*, 235−241.
(12) Woolley, A. T.; Lao, K.; Glazer, A. N.; Mathies, R. A. *Anal. Chem.* **1998**, *70*, 684−688.
(13) Wang, J.; Tian, B.; Sahlin, E. *Anal. Chem.* **1999**, *71*, 3901−3904.
(14) Wang, J.; Tian, B.; Sahlin, E. *Anal. Chem.* **1999**, *71*, 5436−5440.
(15) Wang, J.; Chatrathi, M. P.; Tian, B. *Anal. Chem.* **2001**, *73*, 1296−1300.
(16) Wang, J.; Chatrathi, M. P.; Mulchandani, A.; Chen, W. *Anal. Chem.* **2001**, *73*, 1804−1808.
(17) Henry, C. S.; Zhong, M.; Lunte, S. M.; Kim, M.; Bau, H.; Santiago, J. J. *Anal. Commun.* **1999**, *36*, 305−307.
(18) Martin, R. S.; Gawron, A. J.; Lunte, S. M.; Henry, C. S. *Anal. Chem.* **2000**, *72*, 3196−3202.
(19) Gawron, A. J.; Martin, R. S.; Lunte, S. M. *Electrophoresis* **2001**, *22*, 242−248.
(20) Rossier, J. S.; Roberts, M. A.; Ferrigno, R.; Girault, H. H. *Anal. Chem.* **1999**, *71*, 4294−4299.
(21) Rossier, J. S.; Schwarz, A.; Reymond, F.; Ferrigno, R.; Bianchi, F.; Girault, H. H. *Electrophoresis* **1999**, *20*, 727−731.
(22) Rossier, J. S.; Ferrigno, R.; Girault, H. H. *J. Electroanal. Chem.* **2000**, *492*, 15−22.
(23) Schwarz, M. A.; Galliker, B.; Fluri, K.; Kappes, T.; Hauser, P. C. *Analyst* **2001**, *126*, 147−151.
(24) Chen, D.; Hsu, F.-L.; Zhan, D.-Z.; Chen, C. *Anal. Chem.* **2001**, *73*, 758−762.
(25) Naber, J. F.; Jackson, D. J.; Roussel, T. J., Jr.; Bathlagunda, V.; Crain, M. M.; Pai, R.; Conklin, J. A.; Baldwin, R. P.; Keynton, R. S.; Walsh, K. M. Manuscript in preparation.

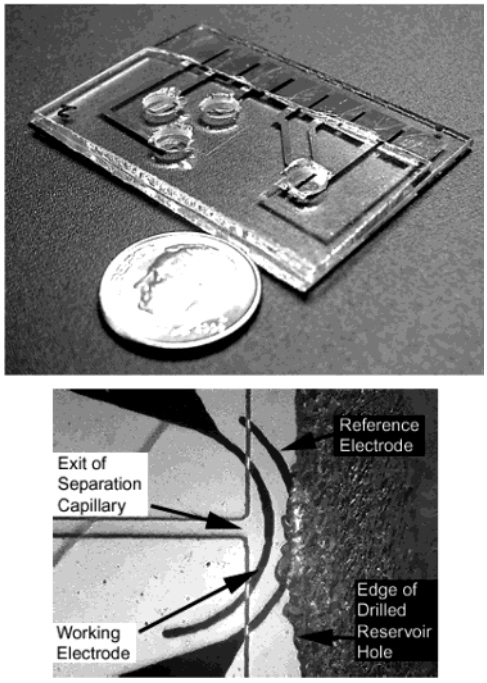

Figure 1. Photographs of (A) entire CE/EC microchip and (B) magnified top view of EC detection cell and electrodes.

photomask that was prepared in-house from an image setter transparency. The exposed chrome layer was then etched using a CEP-200 Micro Chrome etchant so as to expose the glass substrate in the desired electrode regions only. The glass was then etched for 30 s at room temperature in 6:1 buffered oxide etch (BOE, J. T. Baker, Phillipsburg, NJ) to form ∼0.3-μm recessions. This step was performed in order to keep the final surface of the bottom substrate as flat as possible. The electrode material, consisting of a 10-nm adhesion layer of titanium followed by 300 nm of platinum, was then sputtered over the entire glass substrate. Patterning of the electrode material was accomplished by soaking the substrate in acetone and dissolving the underlying positive resist layer. As the resist layer was removed in the solvent, the Ti/Pt electrode material located above it was "lifted off", and only in the exposed recessed patterns did the electrode material remain anchored to the glass substrate. This liftoff process allowed the dual-composition electrodes to be patterned in a single processing step, as opposed to wet etching, which would require multiple selective etching operations. The final process consisted of the removal of the remaining thin chrome layer in the nonelectrode regions using a chrome etchant. A unique aspect of this fabrication sequence was the deliberate recession of the Ti/Pt electrodes into the bottom glass substrate in order to keep the final surface as flat as possible. In our experience, this step was necessary to ensure a high yield of leak-free chips during the final thermal-bonding phase.

Fabrication of the top glass substrate, which contained the microchannels and reservoir openings, involved a slightly more straightforward combination of photolithography, bulk micromachining, and conventional glass drilling. The 20-μm-deep capillary channels were photolithographically patterned and then wet-etched in 6:1 BOE at room temperature for 30 min at an average etch rate of 0.66 μm/min. The resulting CE channels possessed an average width of 50 μm (∼60 μm at the top and 40 μm on the bottom). After the remaining resist and chrome layers were removed, the four reservoir openings ($d = 5$ mm) were then drilled, using a diamond core drill bit, through the top glass substrate at the terminal ends of both channels. An extra hole was drilled ∼1 radius away from the center of the original detection reservoir hole in order to create a slightly larger volume for the EC detection cell.

The top and bottom substrates were then cleaned using a conventional RCA base cleaning procedure (1:1:5 conc NH_4OH/30% H_2O_2/deionized water) of 10 min for the top wafer with the CE channels and only 30 s for the bottom wafer containing the metal electrodes). The two glass pieces were then soaked in deionized water for 2 min and brought into contact under running water. While the glass interface was still wet, the outer surfaces were blown dry with clean nitrogen, and the assembly was immediately moved to an optical microscope for final alignment. After alignment, a weight was placed on the glass wafers to produce a uniform pressure of 50 g/cm^2 over the entire chip. The entire assembly was then transferred to a tube furnace for thermal bonding. The bonding sequence involved a 3 °C/min ramp to 620 °C, followed by a 620 °C soak for 30 min and ending with a 3 °C/min ramp down to room temperature (all in air). Careful ramping of the furnace was required in order to keep the bonded glass assembly from fracturing due to induced thermal stresses. The device was then ready for testing.

Several different configurations of the EC electrodes involving different electrode dimensions and locations on the chip were examined during the course of this work. These are commented on specifically in the Results and Discussion Section. In a few experiments, the microfabricated Pt electrode that served as a pseudoreference electrode was coated electrochemically with an Ag/AgCl layer. This modification was carried out in situ after the microchip device had been assembled as described above. A 1.0 mM $AgNO_3$ solution was placed into the detection reservoir, and the Pt electrode undergoing modification was cycled to a reducing potential (−0.2 to −0.4 V vs Ag/AgCl) and then held for a few minutes until the current had largely dissipated. Subsequently, the $AgNO_3$ solution was replaced with 1.0 mM NaCl, and the potential was cycled back to +0.4 V and again held briefly until the oxidation current decreased to background.

Apparatus. Microchip operation, including both CE and EC functions, was controlled by a miniaturized electronics unit that was designed and custom-made in-house and described in detail in a subsequent instrumentation paper.[25] However, for readers' convenience, a very brief description of the basic design features of this unit is included here. If desired, commercial high-voltage supplies and potentiostats could, of course, be used with little or no difficulty.

High voltages for sample injection and separation in CE were supplied by a two-source power supply powered by four rechargeable AA NiMH batteries capable of independently providing ±250 to ±2000 V across both the separation and injection channels. Because of the comparatively short CE channel lengths, extremely high voltages are generally not required in microchip systems. In the operation of our devices, application of 1000 V was typically sufficient to generate the 250 V/cm electric fields used for both filling the sample channel and for carrying out CE separations. To fill the sample loading channel prior to performing a CE

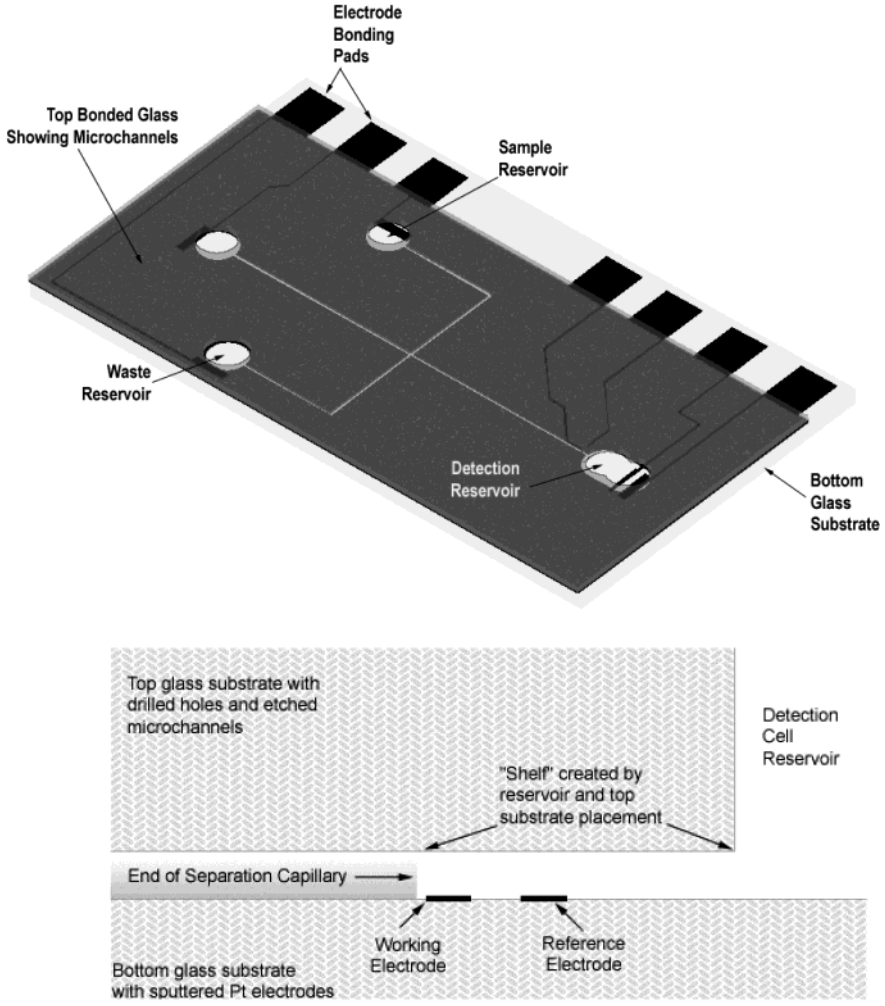

Figure 2. Diagrams showing (A) entire CE/EC device layout and (B) side view of EC detection cell and electrodes.

separation, high voltage (usually −250 V) was applied to the CE electrode in the waste reservoir while CE electrodes in the sample, buffer, and detection reservoirs were all grounded. To initiate sample injection and separation, a positive CE voltage (magnitude determined by the specific separation under study) was applied to the buffer reservoir, and all the other CE electrodes were held at ground.

EC detection was carried out amperometrically with a three-electrode potentiostat constructed from operational amplifiers and various passive components and powered by a single 9 V battery. The potentiostat was capable of applying voltages from +2 to −2 V. Experimental control, including CE and EC operation as well as data collection, was carried out via a laptop computer equipped with controller cards and data acquisition software (LabView, National Instruments, Austin, TX). The high-voltage power supply, the potentiostat, and the data acquisition system all shared the same "common" connection. Although in the laboratory work reported here, this connection was to earth ground, it would of course need to be a "floating" common in any field applications where earth ground is not available.

Reagents. All reagents were purchased from commercial sources and were used as received without further purification. The background electrolyte solution used for all EC and CE experiments consisted of 0.020 M pH 6 phosphate buffer. Analyte solutions were prepared fresh each day by appropriate dilution of stock solutions with this buffer.

RESULTS AND DISCUSSION

Microchip Design. Figure 1 contains photographs of the fabricated CE/EC device, and the diagrams in Figure 2 provide more detailed images showing more precisely the location and orientation of the channels and electrodes. Easy to see in both Figures are the four CE reservoirs (sample, waste, buffer, and detection) that were formed by drilling through the upper glass substrate and the corresponding Pt CE electrodes that were photolithographically patterned onto the bottom plate and located appropriately, one in each of the reservoirs. Shown in more detail in the enlargements of the detection reservoir in Figures 1B and 2B are the smaller Pt EC electrodes (working, reference, and auxiliary), which were also patterned onto the bottom glass piece.

The 20-μm-deep, 50-μm-wide CE channels were essentially the same as those used in most previous lab-on-a-chip CE/EC devices. The length of the separation channel (i.e., from the channel intersection to the detection reservoir) was 1 cm, and to simplify the CE electronics, the lengths of the other three channel segments (from the intersection to the sample, waste, and buffer reservoirs) were the same. This kept the resistance of each

channel segment nearly the same and eliminated the need for special balancing of the potentials applied to each during sample injection and separation operations. Empty channels were filled by placing a small volume of the CE buffer/electrolyte solution in the detection reservoir and allowing capillary action to draw the solution throughout the entire network.

The CE electrodes consisted of 0.3-μm-thick, 2.2-mm-wide, 6.9-mm-long Pt deposits placed in each of the CE reservoirs and located as far as possible from the CE channels in order to minimize the chances for any bubbles that might be formed to disturb fluid flow. EC electrodes consisted of 0.3-μm-thick Pt deposits placed in the detection reservoir only. The working and reference electrodes were 40-μm-wide semicircular Pt "fingers" located in various positions as described below. Figure 1B shows a photograph of one of the optimum arrangements examined, with the working electrode just outside the CE channel exit and the reference nearly 80 μm farther out into the reservoir. The auxiliary electrode was generally larger in size (1 mm wide and 6.9 mm long) and was located out in the detection reservoir, well away from the channel exit and the other EC electrodes. In some cases, the CE cathode was used as the auxiliary electrode with no noticeable change in detector performance. A very attractive characteristic of both the CE and EC electrodes was their relatively high durability. During the course of this work, the only noticeable physical deterioration of successfully deposited Pt electrodes took place during solution exchange operations when a modest vacuum was applied manually to the detection reservoir in order to remove sample or buffer solutions. During these procedures, mechanical stress or mishandling sometimes was seen to produce a liftoff and loss of electrode material. However, with careful handling of the microchip during these operations, such occurrences could be nearly eliminated. Furthermore, normal CE/EC operation (CE voltages of 350 V over the 1-cm separation channel and EC potentials of −0.5 to +1.2 V vs Ag/AgCl) seemed to present no stability problems at all for the electrodes. A possible explanation for this extraordinary ruggedness may be that, unlike other EC microchip devices reported previously, all electrodes here were actually recessed into the bottom glass plate making up the chip. Although this has not been systematically investigated as yet, it is possible that this fabrication step, undertaken in order to facilitate bonding of the two halves of the microchip device, may also have a favorable impact on electrode performance and durability.

EC Detector Design. It was presumed that the specific design of the EC detection cell should have a major effect on the performance of the microchip. In particular, both the physical dimensions of the detection reservoir and the specific placement of the EC and CE electrodes within it were expected to be key structural features that needed to be understood and optimized. With this in mind, it is important to note that the layout illustrated in Figures 1 and 2 depicts the microchip structure that was found to provide optimum analytical performance from among several variations that were examined during the course of this work, and it was this device configuration that was used to generate nearly all of the CE/EC data discussed below. However, before settling on this structure, several alternatives were evaluated experimentally and provided some useful "lessons" in EC detector design. Figure 3 shows an electropherogram obtained for a sample

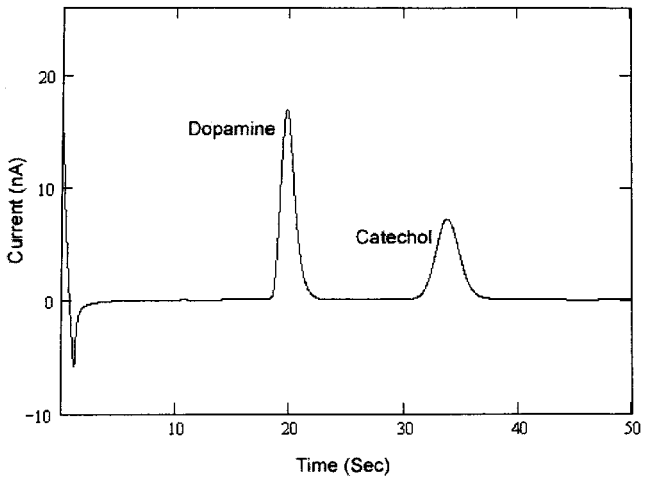

Figure 3. Electropherograms obtained for dopamine (2.2 mM) and catechol (2.3 mM) in pH 6 phosphate buffer for "optimum" microchip configuration. Conditions: CE voltage, 250 V; EC potential, +0.80 V vs Pt wire.

containing the model analytes dopamine and catechol with a microchip whose structure was identical to that illustrated in Figure 1. This electropherogram was initiated by first filling the sample channel with analyte solution (by applying the high voltage across the sample and waste reservoirs) and then switching the high voltage to the separation channel. Upon sample injection, the EC detector current rapidly assumed its steady-state background level, and with the pH 6 buffer solution that was employed, the two compounds were readily separated.

The following design characteristics were found to contribute critically to the analytical performance of the on-chip EC electrodes: (1) the distance between the EC working electrode and the exit of the CE channel, (2) the formation of a "shelf" restricting the height of the detection reservoir in the vicinity of the working electrode, and (3) the nature and positioning of the reference electrode. Each of these design features is considered separately below.

Working Electrode Position. It was determined early on that acceptable performance, not unexpectedly, required a placement of the EC working electrode close to the CE channel exit. Failing this, the observed CE peaks were small and quite broad as a result of rapid three-dimensional diffusion after analyte bands exited the CE channel. Consequently, alignment of the top half of the microchip (containing the CE channels) with the bottom unit (containing the microfabricated electrodes) was always carried out very carefully during the bonding process so that the working electrode was positioned very close to the end of the CE channel so that the leading edge of the 40-μm-wide Pt strip was ~50 μm out from the channel exit.

Detection Reservoir Depth. As illustrated in Figures 1B and 2B, fabrication of CE channels in the upper piece of the microchip assembly included formation of a 20-μm-deep, 6.0-mm-wide opening at the end of the CE channel. As described previously by Wooley et al.,[12] this structure, which essentially formed a "shelf" or "ledge" over the EC working electrode, allowed the dimensions of the CE channel to be increased very rapidly at its exit horizontally in the *x* and *y* directions, thereby decreasing the electrical resistance and CE voltage drop in this postchannel region of the chip. The goal was to minimize the effect of the CE

field on EC detection, because no active decoupling features were designed into the microchip device at this time. This is analogous to the "end-column" or nondecoupled EC detection approach that has been widely employed for EC detection in conventional CE/EC.[26,27] However, at the same time, the "shelf", which kept the depth of the detection chamber the same as that of the CE channel, served to keep the analyte plug well-confined in the *z* dimension until after it had passed the EC working electrode.

The most successful cell configuration (again, that depicted in Figure 2B) was found to be one in which the shelf structure extended beyond the CE channel and the working electrode and then a relatively short distance into the detection reservoir. This arrangement yielded reasonably narrow and well-defined CE peaks for dopamine and catechol and, as will be seen below, allowed effective control of the potential applied to the working electrode. However, use of a shelf that was too long was found to lead to unacceptably large background currents. This was presumably due to poor CE/EC decoupling because of the high residual resistance in the enclosed portion of the detection reservoir.

Interestingly, the fabrication step that established the position of the shelf structure in the detection reservoir was generally also the step that was most difficult to control experimentally. Although virtually all other fabrication was carried out under photolithographic control, the exact placement of the shelf structure with respect to the electrodes was determined by careful manual alignment of the top and bottom halves of the chip under an optical microscope during the bonding operation. This critical step was further complicated by the fact that the edge of the shelf was formed during the mechanical drilling of the access holes to the reservoir and, consequently, was neither perfectly smooth nor perfectly vertical. It is clear that an improved method for forming these access holes and aligning the two halves of the chip would be desirable and is being further investigated by our group.

Reference Electrode. An important issue for any EC-based detection system in CE is the system's ability to control accurately the potential applied to the working electrode. This is an area of particular concern because of the possible interaction between the very high CE voltage and current (usually at the kV and μA levels, respectively) and the much smaller EC voltage and current (typically in the V and nA range). In a few instances, incorporation onto the chip of specific microfabricated features designed to allow the electrical isolation or "decoupling" of the CE and EC operations have been described.[21,22] However, with the exception of a recent report by Chen et al.[24] that described the use of an in-channel Pd metal film decoupler, most lab-on-a-chip devices reported to date have consisted of "end-column" configurations in which there was no active decoupling structure employed. Rather, the working electrode is simply located a short distance outside the physical end of the CE channel and, therefore, outside of the region of highest CE electric field. This end-column approach was employed in our CE/EC microchip devices.

To check the effectiveness of this design, a series of CE experiments was carried out in which dopamine was injected and detected with different potentials applied to the working electrode. Subsequently, a plot of the peak current seen for dopamine as a function of the applied potential was made in order to create a "hydrodynamic voltammogram" (HDV) that could be compared directly to cyclic voltammetry data obtained under the same conditions but without the CE high voltage. A series of such HDVs obtained using one of our integrated CE/EC devices is shown in Figure 4. The HDV shown in curve A was obtained using a Pt pseudoreference electrode that consisted of simply a Pt finger electrode exactly as produced by our microfabrication procedure. Interestingly, this HDV exhibited the plateau behavior indicative of maximum dopamine oxidation at and above +0.5 V and demonstrates essentially the same potential dependence that was observed in corresponding cyclic voltammetry experiments in which a Pt wire was used as the reference electrode. Clearly, there was effective control of the working electrode potential in the microchip device, and further, as seen below, the reproducibility of this simple arrangement, both in the short and long terms, was quite adequate. Also shown in Figure 4 (curve C) is the potential dependence of the background current observed under the dopamine analysis conditions. It is of interest that, even though the microchip device employed a simple Pt working electrode and no deaeration or other special treatment of sample and buffer solutions was performed, a potential range accessible for high quality analytical measurements, from roughly −0.1 to +0.8 V, was quite large.

Despite the fact that the use of a Pt pseudoreference electrode appeared to give fully acceptable performance, it was of interest to construct and evaluate a more conventional reference electrode format. Accordingly, the microfabricated Pt pseudoreference electrode was coated in situ with an electrochemically generated Ag/AgCl layer. Use of this Ag/AgCl-modified surface as the on-chip reference electrode produced the HDV shown in Figure 4, curve B, which was essentially identical to that seen with the Pt pseudoreference except for a 200 mV displacement toward more positive potentials. This shift is exactly what would be expected for the change to a Ag/AgCl reference and, in fact, exactly matched the shift seen for the dopamine wave in cyclic voltammetry when this change in reference electrode was made. Interestingly, the analytical performance of the Ag/AgCl configuration did not appear to be significantly superior to that of the Pt scheme; however, this modification may be important in that it shows the ease and effectiveness with which the composition and properties of the microfabricated metallic electrodes might be changed in situ under electrochemical control.

Finally, the importance of reference electrode placement in the detection reservoir was also examined by using either a microfabricated Pt finger electrode that was located well out into the reservoir at a distance of several mm from the working electrode and CE channel exit or a Pt wire that was simply inserted into the reservoir. In both cases, no drastic change in CE/EC response was seen apart from modest changes in background current and response time. This suggests that, for our CE/EC device, reference electrode positioning may not be a primary factor in optimization of the response of microfabricated CE/EC systems. It should be noted that this observation is counter to what has been reported in some other CE/EC investigations (e.g., refs 12, 28) and certainly merits further study. The reasons for the discrepancy may be related to specific design features of the

(26) Huang, X.; Zare, R. N.; Sloss, S.; Ewing, A. G. *Anal. Chem.* **1991**, *63*, 189−192.

(27) Voegel, P. D.; Baldwin, R. P. *Electrophoresis* **1997**, *18*, 2267−2278.

(28) Klett, O.; Bjorefors, F.; Nyholm, L. *Anal. Chem.* **2001**, *73*, 1909−1915.

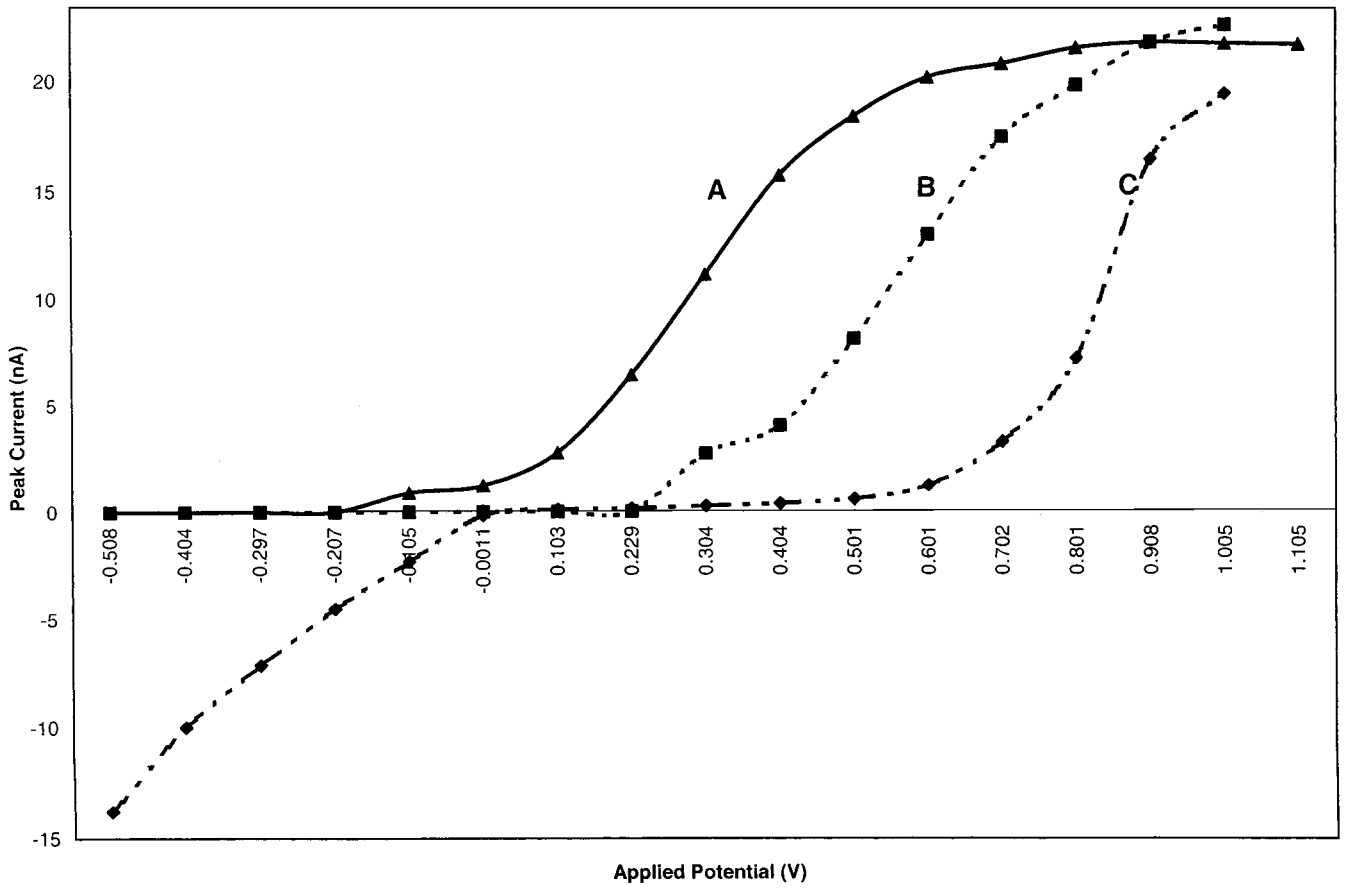

Figure 4. Hydrodynamic voltammograms of (A) dopamine with Pt pseudo-reference electrode, (B) dopamine with Ag/AgCl reference electrode, and (C) phosphate buffer with Pt pseudoreference electrode. Conditions as in Figure 3.

different devices employed by different investigators. An important advantage of the use of microfabrication technology is that this approach makes it feasible to control electrode placement with a high degree of precision and thereby identify and achieve optimum device configuration.

Analytical Performance. Although they are ultimately not the most interesting analytes for lab-on-a-chip systems, the catechols have become the models for characterization of such devices employing EC detection and, therefore, were selected for that purpose here. As mentioned above, Figure 3 shows a typical electropherogram obtained here for such analytes with our optimized microchip design.

As far as actual analyte quantitation was concerned, the limit of detection (signal/noise = 3) was found to be 4.3 μM for dopamine and 4.4 μM for catechol at an applied potential of +0.75 V (vs Pt). Linear response was observed up to 2200 μM for dopamine (y (nA) = 0.0066x (μM) + 0.0404: r^2 = 0.9991) and up to 2300 μM for catechol (y (nA) = 0.0030x (μM) − 0.0774; r^2 = 0.9959). This performance is roughly comparable to that seen for catechols and related analytes at Pt and Au electrodes in previous studies.[18,22,23] (Of course, more sensitive EC detection of these compounds would be expected for a carbon-based working electrode.) However, it should be noted that in the studies reported here, chip design and operation were not conducted with the specific goal of obtaining optimum sensitivity. Rather, the initial priority of our sample injection procedure was maintaining the separation efficiency of the CE system, and accordingly, the sample injection volume was intentionally kept as small as possible. In fact, fluorescence imaging of injected dichlorofluorescein indicated that the sample plug essentially had the same volume as the 50 μm × 50 μm × 20 μm channel intersection, or ~50 pL. Thus, the above detection limits correspond roughly to only 200 amol of dopamine. Moreover, we believe that modest changes in chip fabrication and operating procedures could be implemented to increase this volume—and the associated detection limits—substantially. The separation efficiency seen in Figure 3, represented by the number of theoretical plates, was ~1400 for dopamine and 1130 for catechol (or 140 000 and 113 000 plates/m, respectively, considering the 1-cm length of the separation channel). This efficiency is quite competitive with what has been reported in most microchip studies to date and is related, we believe, to the favorable configuration of the detection cell employed and to the system's ability to form and inject a very well-defined sample plug.

Key to the practical attractiveness of any analytical system is its reproducibility. For the integrated microchip devices here, reproducibility has several different aspects. First, and most simply, there is the short-term repeatability and stability of the response of an individual CE/EC device. For our CE/EC devices, this was evaluated by performing repetitive injections of dopamine and catechol and following the peak currents that resulted. Typical response for nine successive analyses over the course of ~30 min gave relative standard deviations of the dopamine and catechol currents of 1.6 and 2.3%, respectively. This level of reproducibility

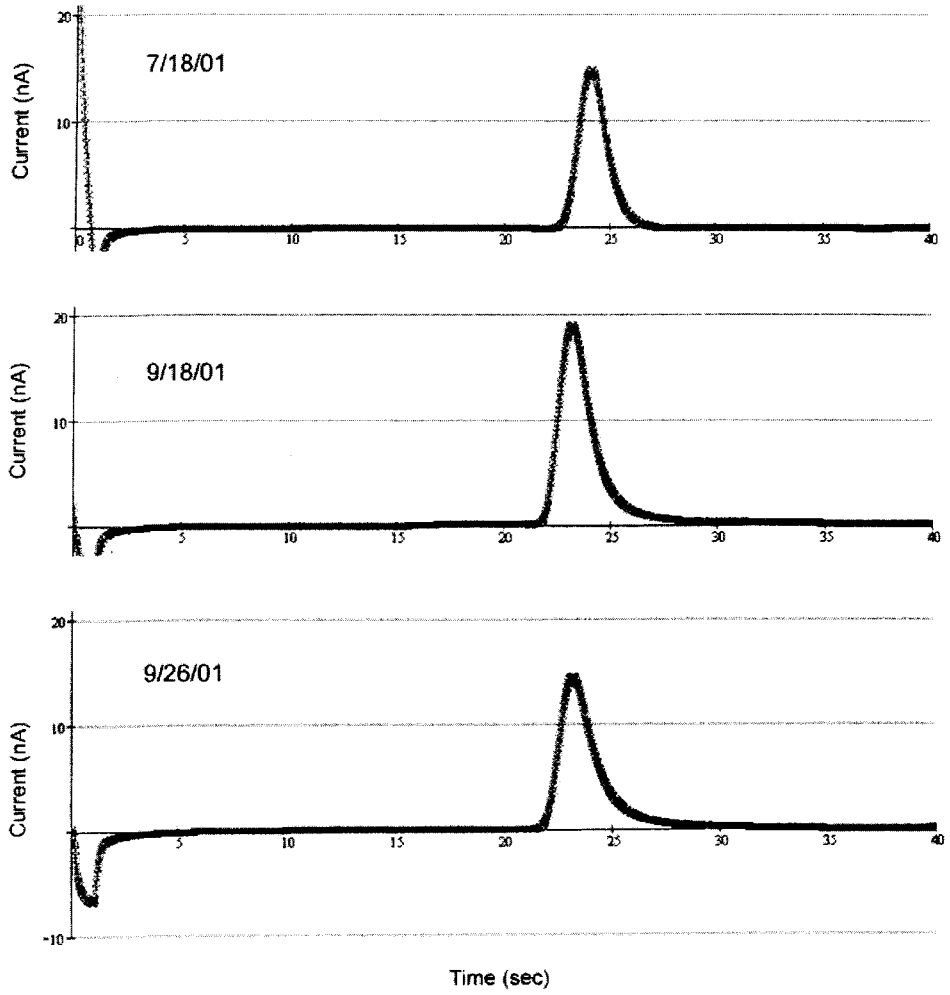

Figure 5. Electropherograms observed for dopamine (2.2 mM) with same microchip device on (A) 7/18/01, (B) 9/18/01, and (C) 9/26/01. Conditions as in Figure 3.

was completely representative for our working microchips which rarely, if ever, exhibited any significant short-term variation in either migration times or electrode response. Compared to conventional CE/EC with ordinary capillary separations, the fully integrated microchip approach in which electrode positions are absolutely fixed was expected to offer this advantage. The second, and probably the more challenging, stability issue has to do with long-term microchip performance over the course of several days or longer. Although the potential exists for mass production of CE/EC microchip devices, our devices in their current stage cannot be considered "disposable" in any realistic sense and need to provide sufficient durability for relatively long-term usage. During the course of this project, some microchip devices were employed in a variety of experiments over relatively long periods. Figure 5 shows the response obtained for dopamine detection for one such chip on three separate occasions spread over a time period of more than two months during which time the chip was used at least 2−3 times/week to carry out a total of several hundred individual CE separations. Although the response was certainly not identical for the experiments shown, the chip performance in terms of migration times and peak currents was very similar throughout this time period, and the chip clearly showed no signs of deterioration.

CONCLUSIONS

For the first time, photolithographic processes have been used to incorporate both CE high-voltage electrodes and EC detection electrodes directly onto the microchip platform. The analytical performance of the resulting devices appears to be comparable to that of previously reported hybrid lab-on-a-chip devices with external CE or EC electrodes or both, with their long-term reproducibility and durability being especially attractive. It seems clear that this approach offers unique potential for precise control of critical electrode characteristics, such as size, shape, and orientation on the microchip. In addition, microfabricated metallic electrodes can be further modified under electrochemical control and, thus, offer routes to improved EC performance and a wide range of analytical applications.

ACKNOWLEDGMENT

This work was supported by the National Science Foundation XYZ-on-a-Chip program under Grant No. CTS-9980831 and by the Department of Energy under Grant No. 46411101095.

Received for review November 16, 2001. Accepted May 7, 2002.

AC011188N